Progress in Natural Science: Materials International 30 (2020) 711–717

Contents lists available at ScienceDirect

Progress in Natural Science: Materials International

journal homepage: www.elsevier.com/locate/pnsmi

Polymer coated nanodiamonds as gemcitabine prodrug with enzymatic sensitivity for pancreatic cancer treatment

Wanying Ye [a], Haijie Han [a,e], Huan Li [a], Qiao Jin [a,**], Yuzhou Wu [b,c], Sabyasachi Chakrabortty [d], Tanja Weil [c,d], Jian Ji [a,*]

[a] MOE Key Laboratory of Macromolecule Synthesis and Functionalization of Ministry of Education, Department of Polymer Science and Engineering, Zhejiang University, Hangzhou, 310027, China
[b] School of Chemistry and Chemical Engineering, Huazhong University of Science and Technology, Wuhan, 430074, China
[c] Max-Planck Institute for Polymer Research, Ackermannweg 10, Mainz, 55128, Germany
[d] Ulm University, Albert-Einstein Allee 11, Ulm, 89077, Germany
[e] Zhejiang Provincial Key Lab of Ophthalmology, Eye Center of the Second Affiliated Hospital, School of Medicine, Zhejiang University, Hangzhou, 310027, China

ARTICLE INFO

Keywords:
Nanodiamonds
Self-assembly
Enzyme-sensitive
Gemcitabine prodrug

ABSTRACT

The fabrication of Gemcitabine (GEM) prodrug was reported to be an effective method to enhance its pancreatic cancer treatment efficiency. Here, a kind of nanocarbon-based materials, nanodiamond (ND), was selected as the nanocarrier of GEM, owing to its outstanding surface properties and non-cytotoxicity. The polyelectrolytes, polyethyleneimine and polyacrylic acid, were used to self-assemble outside ND surface through electrostatic forces, followed by attachment of polyethylene glycol to address better biocompatibility. GEM was conjugated with an enzyme-sensitive peptide gly-phe-leu-gly to build up the controlled release platform. From characterization results of dynamic laser scattering, zeta potential and transmission electron microscope, the significant improvement of ND stability in physiological condition was proved. Non-cytotoxicity of this functionalized ND carriers and cytotoxicity of the prodrug against BxPC-3 pancreatic cancer cells were indicated by methylthiazolyl tetrazolium (MTT) assay. *In vivo* experiments also revealed its superior anticancer effect compared with free GEM treatment. Therefore, the combination of polymer coated NDs with high surface capability and enzyme-responsive intracellular GEM release make it possible to realize higher treatment efficiency on pancreatic tumor therapy.

1. Introduction

Pancreatic cancer is one of the most threatening cancers all over the world due to its high difficulty of diagnosis, high level of malignancy and low survival rate [1]. For those patients who can't suffer surgery, alternative treatment such as chemotherapy that is non-invasive seems preferable to fight against cancer. Gemcitabine (GEM) is reported as an effective and most typical first-line drug for pancreatic cancer therapy [2]. However, the using of GEM is still facing many difficulties due to its specific metabolism and transportation mechanisms [3]. For example, GEM is always metabolized fast in plasma, thus causing the rapid loss of therapeutic activity. Meanwhile, the suppressive expression of several transporters of GEM on cancer cells may block its transportation into cytoplasm [4] and eventually lead to an unsatisfactory treatment efficacy. Therefore, it would be highly desirable to develop new delivery systems to realize efficient and targeted transport of GEM. Recent researches have shown that, conjugated-GEM as a prodrug can effectively prevent GEM from being deaminated by cytidine deaminase (CDA) and enhance its ability of transport into cells [5–8]. Hence, it's expected to introduce nanoparticles as vehicles, so that GEM can be delivered to tumor locations more efficiently according to enhanced permeability and retention (EPR) effect [9,10], and to prevent the drug being pumped out of cells or diffusion out directly [11]. Therefore, the concentration of active GEM in cancer cells can remain above the lethal dose for a longer time and guarantee the treatment efficiency. Moreover, a further step of combining other functions such as active targeted transport [12] and controlled release [13,14] can be achievable based on the prodrug platform.

* Corresponding author.
** Corresponding author.
E-mail addresses: jinqiao@zju.edu.cn (Q. Jin), jijian@zju.edu.cn (J. Ji).

https://doi.org/10.1016/j.pnsc.2020.10.011
Received 10 April 2020; Received in revised form 23 October 2020; Accepted 23 October 2020
Available online 10 November 2020

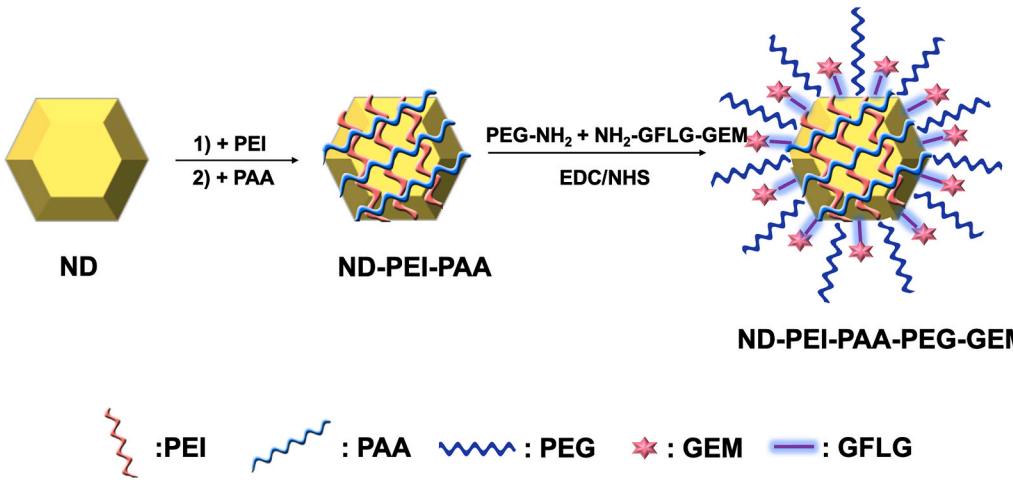

Scheme 1. Scheme of ND-PEI-PAA-PEG-GEM preparation. PEI was firstly adsorbed to NDs by electrostatic force and the surface charge was converted to positive. PAA was then assembled to reform the negative charged carboxyl groups on the surface. These carboxyl groups were activated by EDC/NHS and amidated with PEG-NH2 and NH2-GFLG-GEM.

Nanocarbon materials, such as graphene, carbon nanotube and carbon dots have been widely used in biomedical applications [15–17]. Nanodiamonds (NDs) as one of the nanocarbon-based materials with various advantages, such as its ease of surface modification, low cytotoxicity and high affinity to carry biomolecules [18–20], gradually attracted people's sights in recent years. Several researches reported NDs could be used as drug carrier for cancer therapy [21–24]. Most of these nanodiamond-based nano-drugs were constructed through directly conjugating drug molecules and functional polymers to surface group on nanodiamond (such as carboxyl groups and amino groups). However, the modification capacity was usually limited with the amount of surface active sites. Besides, the greatly consumption of surface charged and hydrophilic groups may directly lead to severe loss of nanoparticle's stability. Thus, it's difficult to align good solubility, biostability and high loading capacity of nanodiamonds only relying on the existing surface groups. To solve the problem, Chen et al. modified hyperbranched polyglycerol to carboxyl groups of nanodiamonds to introduce more –OH groups as reaction sites for further conjugation of drug and better solubility of nanoparticles [25]. In contrast, non-covalent method, such as self-assembly of polyelectrolyte through electrostatic adsorption, is much easier to conduct according to the strong surface charge of carboxylate nanodiamonds [26] and is not limited by the amount of reaction sites. In addition, the assembled polymers on the surface of nanoparticles can also provide sufficient reactive groups for following functionalization process. Consulting to the published methods of constructing polymer-nanoparticle complexes through self-assembly [27,28], it's feasible to amplify reactive groups on NDs by self-assembly method, and ensure the biostability and drug loading capacity simultaneously.

Herein, NDs were used to construct the nano-prodrug of GEM for pancreatic cancer therapy as Scheme 1 shown. Polyethyleneimine (PEI) and polyacrylic acid (PAA) were used to self-assemble outside ND surface through electrostatic forces between each layer. The form of this polyelectrolyte bilayer can help improve the stability of NDs among biological condition, and the increased amount of carboxyl groups can perform as reactive sites for further functionalization of polyethylene glycol (PEG)-NH_2 to obtain better stability. The hydrodynamic sizes of NDs before or after PEI/PAA assembly and PEG conjugation in phosphate buffer saline (PBS) solution and cell culture medium with serum were carefully studied to evaluate the effect of these modifications on NDs' stability among physiological environment. GEM was then conjugated to the surface of the ND-polymer complexes through an enzyme-sensitive peptide gly-phe-leu-gly (GFLG). According to published researches, the nanodiamonds after internalization mainly localized in lysosomes [29–31]. Thus, the peptide can be cleaved by a lysosomal cystein protease, cathepsin B [32,33], which is overexpressed in pancreatic cancer cells [34], thereby GEM can be released inside the cancer cells, preventing the happening of premature release and guaranteeing the activity of GEM. Further characterizations such as dynamic laser scattering (DLS), zeta potential, transmission electron microscope (TEM), methylthiazolyl tetrazolium (MTT) assay and in vivo antitumor experiments were carried out to confirm its biostability, cytotoxicity and antitumor efficacy.

2. Material and methods

2.1. Materials

Nanodiamonds were obtained from Micro-diamant GmbH as a gift. Branched polyethyleneimine (PEI, Mw ~25,000), 1-(3-dimethylaminopropyl)-3-ethylcarbodiimide (EDC), 3-(4,5-dimethylthiazol-2-yl)-2,5-diphenyltetrazolium bromide (MTT), cathepsin B were purchased from Sigma-Aldrich. Polyacrylic acid (PAA, Mw ~3000), N-hydroxysuccinimide (NHS) were purchased from Aladdin. GEM was purchased from Dalian Meilun Biology Technology Co., Ltd., PEG5000-NH_2 was supplied by Seebio Biotech (Shanghai, China), NH_2-GFLG-GEM was obtained from ChinaPeptides (Shanghai, China). MilliQ Water (18.2 MΩ cm^{-1}) was purified with a Millipore MilliQ Academic Water Purification System.

2.2. Assembly of PEI/PAA on nanodiamond surface

2.2.1. PEI assembly

2 g PEI was dissolved in 22 mL deionized water and sonicated for 10 min. The solution was kept stirring at room temperature for 1 h. Meanwhile, 160 μL ND solution (100 mg/mL) was diluted to 24 mL by deionized water and sonicated for 10 min to disperse nanoparticles. Then the ND solution was added to PEI solution dropwise and kept stirring for 3.5 h to assemble PEI around nanodiamonds. The mixture was then centrifuged at 10,000 rpm for 30 min and washed with deionized water for 3 times. The nanoparticles were collected and redispersed in 18 mL deionized water.

2.2.2. PAA assembly

1.2 g PAA was dispersed in 18 mL deionized water and sonicated for 10 min. 1.44 g Na_2CO_3 powder was dissolved in 15 mL deionized water. The Na_2CO_3 solution and PAA solution were mixed and stirred for 1 h to neutralize carboxyl group on PAA and make it negatively charged. Then

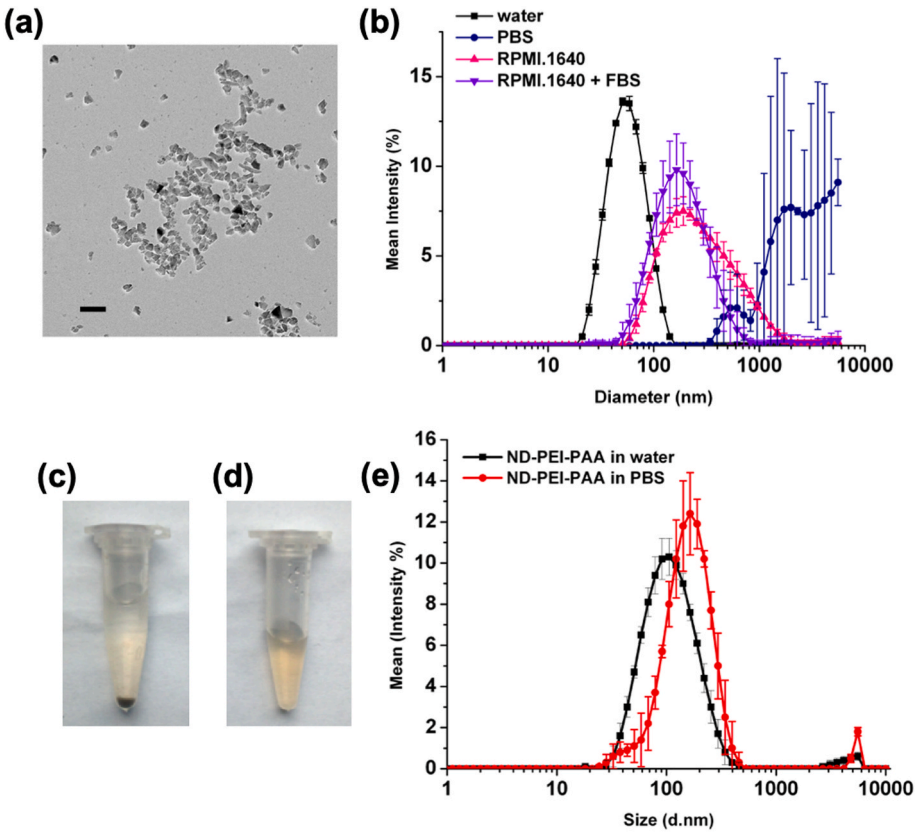

Fig. 1. Characterization of NDs size before or after PEI/PAA assembly. (a) TEM images of raw ND without any modifications, scale bar: 100 nm. (b) Size distributions of ND in water, PBS solution, culture medium and culture medium with 10% FBS. Digital images of ND-PEI-PAA in water (c) and PBS solution (d). (e) Size distribution of ND-PEI-PAA in water and PBS solution.

the obtained ND-PEI solution was sonicated for 10 min and drop to the PAA/Na_2CO_3 solutions. After 3.5 h' stirring, the mixture was centrifuged at 10,000 rpm for 30 min and washed with deionized water for 3 times. The nanoparticles were collected and re-dispersed in 2 mL deionized water.

2.3. Synthesis of ND-PEI-PAA-PEG

1 mL ND-PEI-PAA mentioned above was dispersed in 10 mM phosphate buffer (PB) solution at pH 6.0 and stirred for 30 min for stabilization. 3.4 mg NHS and 6.0 mg EDC were then added to the solution to activate carboxyl groups on the surface of particles. After 30 min, the pH was adjusted to 8.0 by 0.5 M NaOH solution. To conjugate PEG on NDs, 6 mg PEG5000-NH_2 was added to the solution and kept stirring for 24 h at room temperature. The mixture was centrifuged at 10,000 rpm for 30 min and washed with deionized water for 3 times. The nanoparticles were then re-dispersed in 1 mL deionized water and sonicated for 3 min.

2.4. Synthesis of ND-PEI-PAA-PEG-GEM

ND-PEI-PAA-PEG-GEM was prepared by the similar method with ND-PEI-PAA-PEG. 1.5 mL ND-PEI-PAA solution was dispersed in 4.5 mL PB solution at pH6.0 for 30 min 3.4 mg NHS and 6.0 mg EDC was added to the solution to activate carboxyl groups for 30 min 2.4 mg NH_2-GFLG-GEM and 4.3 mg PEG5000-NH_2 was added after adjusting the solution pH to 8.0 with 0.5 M NaOH solution. The mixture was kept stirring for 24 h to form amide bond. The nanoparticles were separated by centrifugation at 10,000 rpm for 30 min and washed with deionized water for 3 times. The sediment was re-dispersed in 1.5 mL deionized water and sonicated for 3 min.

2.5. Characterization

The Dynamic Light Scattering and zeta potential were measured by a Zetasizer Nano-ZS from Malvern Instruments equipped with a He−Ne laser with a wavelength of 633 nm at 25 °C using a detection angle of 173°. Transmission electron microscopy images were taken on a HT7700 TEM (HITACHI, Japan) operated at an accelerating voltage of 100 kV.

2.6. Measurement of enzyme-sensitive GEM release

200 μL ND-PEI-PAA-PEG-GEM and 10 μL cathepsin B was added to 800 μL PBS buffer at pH 5.5. The nanoparticles were incubated at 37 °C for 24 h and then separated by centrifugation at 10,000 rpm for 30 min. The concentration of dissociative fragments was analyzed by HPLC with mobile phase of water and acetonitrile (80:20, v/v) containing 0.1% TFA at 1 mL/min and detected at 280 nm.

2.7. Cell culture

The human pancreatic cancer cell line BxPC-3 cells purchased from KeyGen BioTECH (Nanjing, China) were cultured in RPMI 1640 containing 10% fetal bovine serum (FBS), and grown at 37 °C with 5% CO_2.

2.8. In vitro cytotoxicity assay

The cytotoxicity of free GEM, ND-PEI-PAA-PEG and ND-PEI-PAA-PEG-GEM was measured by MTT assay. The pancreatic cancer cells BxPC-3 were incubated in 96-well plates for 24 h to adhere bottom with the density of 5000 cells per well. GEM and ND-PEI-PAA-PEG-GEM were dissolved in culture medium RPMI1640 + 10% FBS with gradient GEM

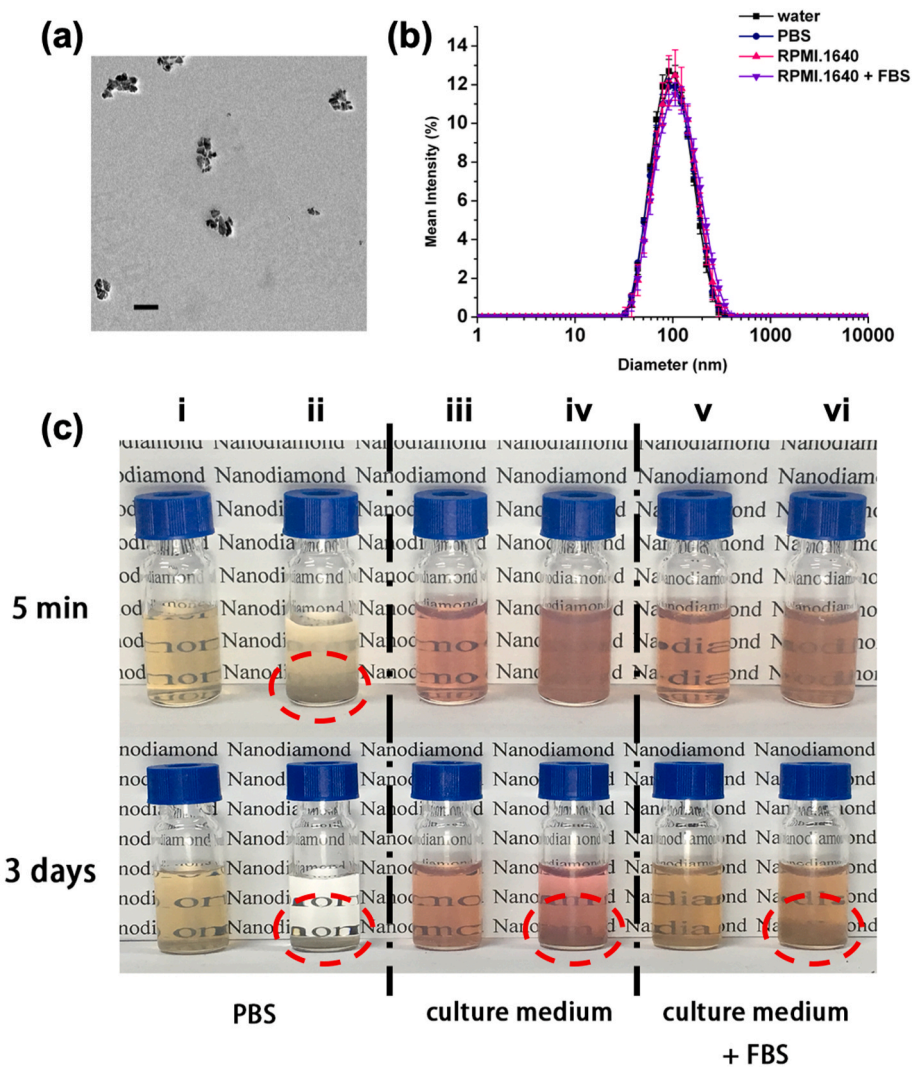

Fig. 2. (a) TEM image of ND-PEI-PAA-PEG-GEM, scale bar: 100 nm. (b) Size distribution of ND-PEI-PAA-PEG-GEM in water, PBS solution, culture medium and culture medium with 10% FBS. (c) Photo of 1 mg/mL ND-PEI-PAA-PEG-GEM (i, ii, v) and raw ND (ii, iv, vi) dispersed in PBS (i, ii), culture medium (ii, iv) and culture medium with 10% FBS (v, vi) after 5 min or 3 days placement. The sediments at bottom were circled with red dash line.

concentration at 0.2, 0.5, 1, 2, 5 μg/mL respectively. ND-PEI-PAA-PEG was also dissolved in the same medium with equivalent ND concentration to ND-PEI-PAA-PEG-GEM. 200 μL of each sample was added to per well, and other wells were filled by 200 μL fresh culture medium as control. The cells were incubated with the samples for 72 h and then the previous culture medium was replaced by 200 μL MTT solution of culture medium (0.5 mg/mL) in dark. After another 4 h' incubation, the culture medium was removed and 150 μL DMSO was added per well to dissolved the purple crystals generated by live cells. When the crystals were totally dissolved after 15 min, the plate was placed in a MUtiskan Spectrum microplate reader to record the absorbance at 570 nm.

2.9. In vivo anti-tumor activity

All animal experiments were performed according to the "Principles of Laboratory Animal Care" (NIH publication NO. 86–23, revised 1985) and the guidelines for Animal Care and Use Committee, Zhejiang University. Healthy male BALB/c nude mice (5 weeks old, weight around 15 g) purchased from the animal center of Zhejiang Academy of Medical Sciences, were used as a tumor model. BxPC-3 cells (2×10^6) in 0.1 mL of PBS were injected directly into nude mice. When the volume of tumors reached around 100 mm^3, the mice were randomly divided into three experimental groups. Then, 150 μL of PBS, free GEM (8 mg/kg equivalent to GEM) and ND-PEI-PAA-PEG-GEM (8 mg/kg equivalent to GEM) were injected through tail veins for four times twice per week, respectively. Meanwhile, tumor growth and body weight of the mice were checked twice weekly. The tumor size was measured using a caliper, and the tumor volume was calculated as $1/2 \times \text{length} \times \text{width}^2$.

2.10. Histological analysis

For histology, tumor tissues were extracted from those mice after tail intravenous injection for 24 h. The tumor tissues were fixed by 4% formaldehyde for 24 h and embedded in paraffin and then sectioned to 5 μm. Then the sections were stained with Hematoxylin and Eosin stains (H&E). To evaluate the apoptosis, the sections were determined with a TdT-mediated dUTP nick end-labeling (TUNEL) assay (according to the manufacturer's instructions).

3. Results

3.1. Characterization of the polymer-complexed ND stability in biological environment

The diameters of pristine NDs in water, PBS and cell culture medium, which used to imitate the saline condition and complicated component

Table 1
Characterizations of nanodiamonds in hydrodynamic size and zeta potential. (Size distributions of these particles are shown in supporting information, Figure S1.)

Particles	Diameter (nm) ± Std Dev	PDI	Zeta potential (in 10 mM PB 7.4) (mV) ± Std Dev
ND	47.8 ± 0.2	0.183	−34.2 ± 0.2
ND-PEI	85.6 ± 0.2	0.159	+9.3 ± 0.1
ND-PEI-PAA	83.6 ± 0.9	0.134	−37.1 ± 3.4
ND-PEI-PAA-PEG	91.3 ± 0.3	0.140	−31.3 ± 2.2
ND-PEI-PAA-PEG-GEM	91.5 ± 0.3	0.169	−27.2 ± 1.5

in the biological environment, were characterized by DLS and TEM first. The results showed that NDs were well dispersed in water with the hydrodynamic diameter of 47.8 nm and PDI of 0.183. Some of the NDs were observed as clusters of 2–3 single nanoparticles in TEM images, while part of the nanoparticles aggregated to larger clusters above 200 nm (Fig. 1a). This inhomogeneous size distribution was not expected in drug delivery systems [35]. Besides, the size distribution and dispersion performance of NDs also showed dramatic change in different disperse mediums (Fig. 1b). Bare NDs immediately aggregated and formed sediments in PBS (Fig. 1c), probably because of the high salt concentration that may shield the electrostatic force between nanoparticles. Owing to the high negative zeta potential of NDs at about −34.2 mV, no apparent precipitation occurred in culture medium, but the hydrodynamic diameter also increased to 209.6 nm. Irreversible sediments eventually formed after 3 days placement (Fig. 2). Similar results were observed in culture medium with 10% fetal bovine serum (FBS), while the average size was slightly smaller (157.7 nm). It can be explained when considered the adsorption of proteins that may provide stronger repulsive interactions between nanoparticles. Nevertheless, precipitations were found 3 days later as well.

Taking account of the strong aggregation of NDs in physiological environment, appropriate surface modifications were expected. According to the published method [36], positive-charged PEI was selected to coat NDs through electrostatic force considering the negative surface property of NDs. NDs dispersed in water were mixed with PEI solution during stirring by dropwise addition. The conversion of zeta potential from negative to positive on ND surface demonstrated the successful self-assembly of PEI. PAA with negative charge (when pH > 7) was then added to assemble and form an outer-layer with a large number of carboxyl groups, which turned the surface charge back to negative again. The DLS and zeta potential results of each step products were listed in Table 1 and Figure S1. The size distributions of NDs before or after the self-assembly of PEI/PAA were both mono-disperse, with the mean diameter increasing from 47.8 nm to 83.6 nm, and PDI decreasing from 0.183 to 0.134. It is hypothesized that the PEI/PAA layers outside encapsulated more than one original ND particle, which caused the raise of mean diameter, while the lower PDI may be caused by the separation of large cluster after coating of the polyelectrolyte layers. What's more, the magnitude of zeta potential of ND-PEI-PAA in PB solution at pH 7.4 was increased compared with ND, which means the amount of carboxyl groups on the nanoparticles was amplified after the assembly of PEI/-PAA. For one thing, the increasing number of carboxyl groups can provide more reactive sites for further reactions and enhanced the conjugation efficiency. For another, compared with raw NDs stabilized only by negative carboxyl groups, polyelectrolyte bilayers with both positive and negative charges possess an overwhelming capability to keep nanoparticles stable in various circumstances. From DLS measurement, the size distribution of ND-PEI-PAA was found nearly unchanged even after 1 month (Figure S2), which demonstrated the excellent stability of the complexes and ensured the ease of further design. In addition, ND-PEI-PAA dispersed in PBS also kept clear without any sediment formation (Fig. 1d), and the average diameter only showed a little increase (Fig. 1e).

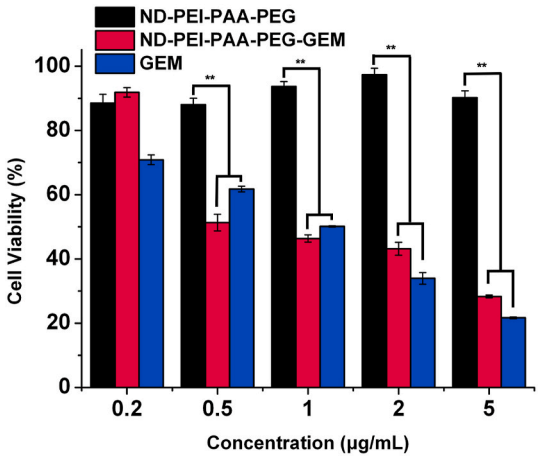

Fig. 3. MTT assay of nanodiamond-conjugated GEM and free GEM, comparing with nanodiamonds without drug, which showed the cytotoxicity of ND-PEI-PAA-PEG-GEM and nontoxicity of ND-PEI-PAA-PEG. Error bars indicate SD (n = 3), **p < 0.01.

However, only the assembly of PEI/PAA was still insufficient to prevent aggregation of NDs among serum condition. Thus, PEG-NH_2 was then linked to ND-PEI-PAA through amidation reaction to prevent the nonspecific adsorption of proteins in physiological environment. The hydrodynamic diameters and PDI of ND-PEI-PAA-PEG was 91.3 nm and 0.140, only slightly larger than ND-PEI-PAA. Subsequently, NH_2-GFLG-GEM was also conjugated through amide bond. The unreacted NH_2-GFLG-GEM was collected from the upper solution after centrifugation and analyzed by HPLC to determine the grafting ratio. The result showed that 19.45% (GEM/ND, wt./wt.) GEM was conjugated to NDs. The size was also similar to that of ND-PEI-PAA-PEG, with the diameters of 91.5 nm and PDI of 0.169 respectively, fulfilling the size demand for EPR effect. Through TEM image, it was ensured that the assembly of PEI/PAA and covalent decoration step didn't change the morphology of ND particles, only transformed the dispersion state into larger cluster form (Fig. 2a). The size distribution of ND-PEI-PAA-PEG-GEM also exhibited a similar shape, only with an apparent shift of peak position compared to raw NDs (Figure S3). To further prove its resistance toward saline condition and protein adsorption, the nano-prodrug was dispersed in PBS and culture medium with or without 10% FBS. In sharp contrast with the raw ND group, NDs with the series of modifications showed excellent dispersiveness in all these mediums. No aggregations were found even after 3 days (Fig. 2c (i, ii, v)), compared with raw ND (Fig. 2c (ii, iv, vi)). The size distribution also retained perfectly (Fig. 2b), which indicated the improvement of colloidal stability in physiological environment with the help of PEG attachment.

3.2. Drug release and cytotoxicity of the ND-polymer complex prodrug

The drug release experiment in vitro was then processed. ND-PEI-PAA-PEG-GEM was dispersed in PBS solution at pH 5.5 with cathepsin B to modulate lysosome environment. The small molecule peptide-conjugated drug NH_2-GFLG-GEM was set as control. The mixtures were incubated for 24 h and then separated by centrifugation. The detached GEM was analyzed by HPLC. It was indicated that 13.85% GEM was released from ND surface, while for random NH_2-GFLG-GEM molecules, 35.28% peptides were cleaved. The slower hydrolysis was probably due to the existence of PEG that may interfere the combination of enzyme and active site in GFLG.

The cytotoxicity of ND-PEI-PAA-PEG-GEM was next measured by MTT assay. The treatment effects toward pancreatic cancer cells (BxPC-3 cells) of free GEM and ND-conjugated GEM were compared. Meanwhile, ND-PEI-PAA-PEG with equivalent ND concentration was also

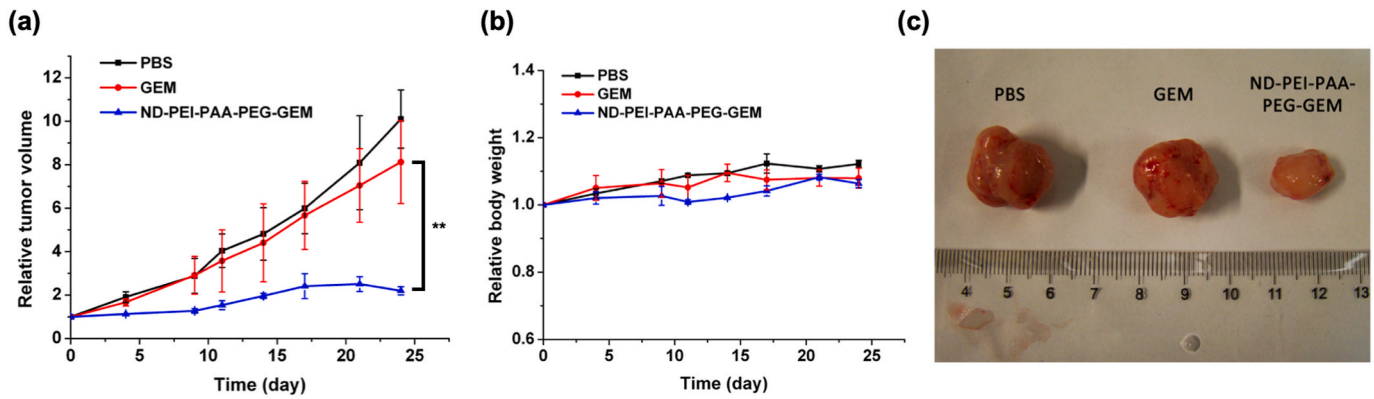

Fig. 4. Antitumor effect of ND-PEI-PAA-PEG-GEM. (a) The growth ratio of tumors in nude mice treated by PBS, GEM and ND-PEI-PAA-PEG in 24 days. (b) Body weight of nude mice treated with ND-PEI-PAA-GEM, PBS and free GEM, respectively. (c) Photo of tumors extracted from the mice treated by PBS, free GEM and ND-PEI-PAA-PEG-GEM (left to right) after 24 days culture.

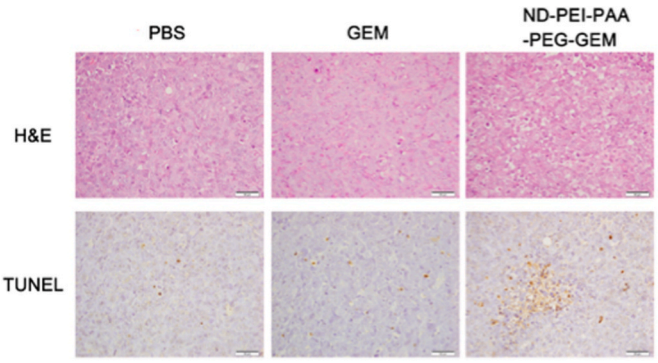

Fig. 5. Immunohistochemical analysis of tumor tissue sections treated by PBS, free GEM and ND-PEI-PAA-PEG-GEM (left to right column), stained with H&E and TUNEL (upper to lower row).

tested to show the biosafety of this nano-carrier. All the samples were dispersed in culture medium containing 10% FBS and cultured with BxPC-3 cells in a 96-well plate for 72 h. Cells with fresh culture medium without drug or nanoparticles were set as control. It was found that the cytotoxicity of GEM carried by NDs was approximate to that of free GEM with the same dose. Moreover, the viability of cells treated with ND-PEI-PAA-PEG at any concentration in the experiment range were all around 90%, which means NDs before conjugating GEM exhibited an ideal biosafety toward cells (Fig. 3).

3.3. *Anti-tumor efficacy of the ND-polymer complex prodrug*

The antitumor effects of ND-PEI-PAA-PEG-GEM nanoparticles were evaluated using BxPC-3 tumor-bearing nude mice as the xenograft tumor model subsequently. Free GEM and ND-PEI-PAA-PEG-GEM with equivalent GEM dose of 8 mg/kg were intravenously injected to mice every 3–4 days, while PBS was injected as control. The change of tumor size observed every 3–4 days revealed that the antitumor effect of ND-conjugated GEM was significantly better than free GEM (Fig. 4a), corresponding to the excised tumor size (Fig. 4c). The reasons of the enhanced effect are presumed to be the passive targeted function due to EPR effects of nanoparticles, and the protection of GEM from being metabolized by construction of prodrug. The variation tendency of body weight both in experiment group and control groups showed no significant differences, proving the biosafety of this prodrug (Fig. 4b).

Additionally, histological analyses of tumor samples were examined (Fig. 5). From the tumor tissue sections stained by H&E, it's obvious to find that the number of apoptotic cells in section treated by ND-PEI-PAA-PEG-GEM was much larger than those treated by PBS and free GEM. According to TUNEL stained sections, only a few cell apoptosis was found in PBS and free GEM samples, while the apoptosis in ND-PEI-PAA-PEG-GEM treated samples was much more apparent, revealing the better antitumor effects of this ND-based prodrug.

4. Conclusions

A new platform for GEM delivery based on nanodiamonds was constructed. Raw NDs were firstly coated by PEI/PAA bilayers through electrostatic force to enhance the stability in saline and to amplify the amount of surface carboxyl groups as reactive sites simultaneously. PEG was then grafted to improve the antifouling property toward proteins, which is the prerequisite to realize long-time circulation and accumulation of nanoparticles in tumor tissue through EPR effect. GEM was conjugated to NDs by enzyme-sensitive peptide GFLG to obtain the intracellular control release feature. The diameter of NDs after these modifications can keep around 90 nm, which is ideal for passive targeted by EPR effect. The cytotoxicity assays indicate that GEM carried by NDs shows similar efficiency to kill pancreatic cancer cells compared with free GEM at equivalent dose in vitro, while ND-PEI-PAA-PEG reveals nearly no cytotoxicity. From in vivo experiments, the antitumor effect of ND-PEI-PAA-PEG-GEM is significantly better than free GEM, demonstrating our design of this ND-based GEM delivery system effectively improves the pancreatic tumor treatment efficiency. In summary, our method provides a novel form of GEM prodrug using nanodiamonds, to achieve higher efficiency of pancreatic cancer chemotherapy. It's promising to further combine diagnosis function by using fluorescent nanodiamonds, and active targeting function to build the theranostic platform in the future.

Declaration of competing interest

The authors declare that they have no known competing financial interests or personal relationships that could have appeared to influence the work reported in this paper.

Acknowledgements

Financial support from the National Natural Science Foundation of China (51573160), the Science and Technology Program of Zhejiang Province (Grant No. 2016C04002) and the Fundamental Research Funds for the Central Universities (2016QNA4033) is gratefully acknowledged. The authors would like to thank the support from EU Horizon 2020 hyperdiamond.

Appendix A. Supplementary data

Supplementary data to this article can be found online at https://doi.org/10.1016/j.pnsc.2020.10.011.

References

[1] T. Kamisawa, L.D. Wood, T. Itoi, K. Takaori, Lancet 388 (2016) 73–85, https://doi.org/10.1016/S0140-6736(16)00141-0.
[2] E. Moysan, G. Bastiat, J.-P. Benoit, Mol. Pharm. (2013) 430–444, https://doi.org/10.1021/mp300370t.
[3] L.H. Reddy, P. Couvreur, Curr. Pharmaceut. Des. 14 (2008) 1124–1137, https://doi.org/10.2174/138161208784246216.
[4] Y. Nakano, S. Tanno, K. Koizumi, T. Nishikawa, K. Nakamura, M. Minoguchi, et al., Br. J. Canc. 96 (2007) 457–463, https://doi.org/10.1038/sj.bjc.6603559.
[5] X. Chen, W. Teng, Q. Jin, J. Ji, Colloids Surf., B 181 (2019) 94–101, https://doi.org/10.1016/j.colsurfb.2019.05.038.
[6] Haiping Zhong, J. Mu, Y. Du, Z. Xu, Y. Xu, N. Yu, et al., Biomacromolecules 21 (2020) 803–814, https://doi.org/10.1021/acs.biomac.9b01493.
[7] H. Han, D. Valdepérez, Q. Jin, B. Yang, Z. Li, Y. Wu, et al., ACS Nano 11 (2017) 1281–1291, https://doi.org/10.1021/acsnano.6b05541.
[8] L.-H. Liu, W.-X. Qiu, B. Li, C. Zhang, L.-F. Sun, S.-S. Wan, et al., Adv. Funct. Mater. 26 (2016) 6257–6269, https://doi.org/10.1002/adfm.201602541.
[9] Y. Matsumura, H. Maeda, Canc. Res. 46 (1986) 6387–6392.
[10] H. Maeda, J. Contr. Release 164 (2012) 138–144, https://doi.org/10.1016/j.jconrel.2012.04.038.
[11] S. Nie, Y. Xing, G.J. Kim, J.W. Simons, Annu. Rev. Biomed. Eng. 9 (2007) 257–288, https://doi.org/10.1146/annurev.bioeng.9.060906.152025.
[12] B. Sivakumar, R.G. Aswathy, Y. Nagaoka, S. Iwai, K. Venugopal, K. Kato, et al., RSC Adv. 3 (2013), https://doi.org/10.1039/c3ra42645a, 20579–20.
[13] L. Xu, Y. Yang, M. Zhao, W. Gao, H. Zhang, S. Li, et al., J. Mater. Chem. B. 6 (2018) 1076–1084, https://doi.org/10.1039/C7TB02479G.
[14] S. Bai, Y.-E. Gao, X. Ma, X. Shi, M. Hou, P. Xue, et al., Carbohydr. Polym. 182 (2018) 235–244, https://doi.org/10.1016/j.carbpol.2017.11.028.
[15] D. Plachá, J. Jampilek, Nanomaterials 9 (2019) 1758–1794, https://doi.org/10.3390/nano9121758.
[16] M.I. Sajid, U. Jamshaid, T. Jamshaid, N. Zafar, H. Fessi, A. Elaissari, Int. J. Pharm. 501 (2016) 278–299, https://doi.org/10.1016/j.ijpharm.2016.01.064.
[17] Y. Song, S. Zhu, B. Yang, RSC Adv. 4 (2014) 27184–27200, https://doi.org/10.1039/C3RA47994C.
[18] K. Turcheniuk, V.N. Mochalin, Nanotechnology 28 (2017) 252001–252028, https://doi.org/10.1088/1361-6528/aa6ae4.
[19] J.M. Rosenholm, I.I. Vlasov, S.A. Burikov, T.A. Dolenko, O.A. Shenderova, J. Nanosci. Nanotechnol. 15 (2015) 959–971, https://doi.org/10.1166/jnn.2015.9742.
[20] A. Krueger, D. Lang, Adv. Funct. Mater. 22 (2012) 890–906, https://doi.org/10.1002/adfm.201102670.
[21] W. Zhao, S. Wei, H. Zhao, Y. Li, R. Wu, J. Wang, Diam. Relat. Mater. 77 (2017) 171–180, https://doi.org/10.1016/j.diamond.2017.07.003.
[22] L. Fusco, E. Avitabile, V. Armuzza, M. Orecchioni, A. Istif, D. Bedognetti, et al., Carbon 160 (2020) 390–404, https://doi.org/10.1016/j.carbon.2020.01.003.
[23] M. Lu, Y.-K. Wang, J. Zhao, H. Lu, M.H. Stenzel, P. Xiao, Macromol. Rapid Commun. 37 (2016) 2023–2029, https://doi.org/10.1002/marc.201600344.
[24] H. Lai, M. Lu, H. Lu, M.H. Stenzel, P. Xiao, Polym. Chem. 7 (2016) 6220–6230, https://doi.org/10.1039/C6PY01188H.
[25] L. Zhao, Y.-H. Xu, T. Akasaka, S. Abe, N. Komatsu, F. Watari, et al., Biomaterials 35 (2014) 5393–5406, https://doi.org/10.1016/j.biomaterials.2014.03.041.
[26] X. Zhang, C. Fu, L. Feng, Y. Ji, L. Tao, Q. Huang, et al., Polymer 53 (2012) 3178–3184, https://doi.org/10.1016/j.polymer.2012.05.029.
[27] S. Labala, P. Kumar, Mandapalli, A. Kurumaddali, V.V.K. Venuganti, Mol. Pharm. 12 (2015) 878–888, https://doi.org/10.1021/mp5007163.
[28] F. Fan, L. Wang, F. Li, Y. Fu, H. Xu, ACS Appl. Mater. Interfaces 8 (2016) 17004–17010, https://doi.org/10.1021/acsami.6b04998.
[29] O. Faklaris, V. Joshi, T. Irinopoulou, P. Tauc, M. Sennour, H. Girard, et al., ACS Nano (2009) 3955–3962, https://doi.org/10.1021/nn901014j.
[30] R. Eldawud, M. Reitzig, J. Opitz, Y. Rojansakul, W. Jiang, S. Nangia, et al., Nanotechnology 27 (2016), https://doi.org/10.1088/0957-4484/27/8/085107, 085107–12.
[31] X.-Q. Zhang, R. Lam, X. Xu, E.K. Chow, H.-J. Kim, D. Ho, Adv. Mater. 23 (2011) 4770–4775, https://doi.org/10.1002/adma.201102263.
[32] J. Wang, N. Li, L. Cao, C. Gao, Y. Zhang, Q. Shuai, et al., J. Mater. Chem. B. 8 (2020) 1157–1170, https://doi.org/10.1039/C9TB02130B.
[33] H. Han, W. Teng, T. Chen, J. Zhao, Q. Jin, Z. Qin, et al., Chem. Commun. 53 (2017) 9214–9217, https://doi.org/10.1039/c7cc04872f.
[34] K. Hirai, M. Yokoyama, G. Asano, S. Tanaka, Hum. Pathol. 30 (1999) 680–686, https://doi.org/10.1016/S0046-8177(99)90094-1.
[35] Y. Wu, A. Ermakova, W. Liu, G. Pramanik, T.M. Vu, A. Kurz, et al., Adv. Funct. Mater. 25 (2015) 6576–6585, https://doi.org/10.1002/adfm.201502704.
[36] C. Boyer, A. Bousquet, J. Rondolo, M.R. Whittaker, M.H. Stenzel, T.P. Davis, Macromolecules 43 (2010) 3775–3784, https://doi.org/10.1021/ma100250x.